CAUCHY – Jurnal Matematika Murni dan Aplikasi
Volume 11 (1) (2026), Pages 224-238
p-ISSN: 2086-0382; e-ISSN: 2477-3344

Modeling the Dynamics of Tuberculosis-Diabetes Mellitus Coinfection with an Optimal Control Approach

Muna Afdi Muniroh*, Kresna Oktafianto, and Eriska Fitri Kurniawati

Department of Mathematics, Faculty of Mathematics and Natural Sciences, University of PGRI Ronggolawe, Tuban, East Java, Indonesia

Abstract

Tuberculosis–Diabetes Mellitus (TB–DM) coinfection increases morbidity, treatment failure, and healthcare costs. This study analyzes TB–DM transmission dynamics and identifies effective prevention strategies using a ten-compartment mathematical model that distinguishes non-diabetic and diabetic populations, each classified into susceptible, latent, active, treatment, and recovered classes. Numerical analysis verifies that the disease-free equilibrium is stable when the basic reproduction number is less than one, whereas an endemic equilibrium exists when it exceeds one. Using baseline parameter values, the reproduction number is estimated as 3.592, indicating persistent TB–DM transmission. An optimal control framework is formulated to evaluate two time-dependent interventions: reducing TB transmission through case detection and contact tracing, and preventing diabetes onset in non-diabetic individuals through metabolic monitoring. Numerical simulations demonstrate that the combined implementation of both control strategies significantly reduces TB–DM incidence while minimizing intervention costs. These findings support the importance of integrated, time-varying TB–DM control programs for public health.

Keywords: tuberculosis, diabetes mellitus, mathematical model, optimal control

1. Introduction

Tuberculosis (TB) remains a serious global health problem despite intensive prevention, detection, and treatment efforts. The disease is caused by infection with the bacterium Mycobacterium tuberculosis (Mtb), which spreads through the air [1]. TB infection consists of two stages: latent TB and active TB. Individuals with latent TB do not show symptoms and do not transmit the disease, while individuals with active TB show symptoms and have the potential to transmit the disease. If latent TB is left untreated, there is a possibility that the infection will develop into active TB. According to the WHO, five countries account for 56% of global TB cases: India (26%), Indonesia (10%), China (6.8%), the Philippines (6.8%), and Pakistan (6.3%).

The treatment of Mtb infection typically lasts between four and nine months, depending on the treatment regimen [2]. Standard therapy for drug-susceptible TB consists of isoniazid, rifampicin, pyrazinamide, and ethambutol. Poor adherence to treatment increases the risk of mortality, relapse, and the emergence of drug-resistant TB strains. These adverse outcomes are more prevalent among individuals with compromised immune systems, particularly those

*Corresponding author. E-mail: munaafdimuniroh@gmail.com

Submitted: November 16, 2025 Reviewed: December 22, 2025 Accepted: January 26, 2026
DOI: https://doi.org/10.18860/cauchy.v11i1.37539

with diabetes mellitus (DM). DM is a major comorbidity that increases susceptibility to TB and worsens disease outcomes, with diabetic individuals facing a two- to threefold higher risk of developing active TB compared with non-diabetic individuals [3].

Mathematical models play an important role in understanding the dynamics of infectious disease spread, including TB-DM coinfection, through nonlinear differential equation systems. Several previous studies have examined the relationship between TB and DM. [4] constructed a TB-DM model considering immunization factors, while [5] discussed TB-DM modeling in Indonesia. [6] assumed the possibility of natural healing for DM patients infected with active TB. The transmission dynamic of TB among diabetic patients in India was described by [7]. Furthermore, [8] conducted an optimal control analysis on a TB spread model with a case study in the city of Surabaya. [9] employed Pontryagin's Minimum Principle together with the forward–backward sweep procedure to determine the optimal control solutions. In addition, [10] incorporated six optimal controls in the TB–DM co-dynamics model: healthy lifestyle (diabetes prevention), prevention of diabetes complications through regular check-ups and personal hygiene, TB treatment for non-diabetic individuals, TB treatment for diabetic individuals without complications, TB treatment for diabetic individuals with complications, and prevention measures against activation of TB.

To better understand TB–DM coinfection dynamics and to identify effective control strategies, this study extends the TB model proposed by [6]. The proposed model explicitly distinguishes TB treatment compartments for non-diabetic and diabetic individuals, reflecting differences in treatment response and clinical management between these groups [11]. The primary objective of this study is not only to analyze the disease dynamics, but also to determine optimal control strategies that reduce TB–DM transmission while accounting for implementation costs. Specifically, two control measures are considered: a TB transmission prevention control incorporating case detection, isolation, contact tracing, behavioral education, and environmental protection measures, and a DM prevention control for individuals at risk of or affected by TB focusing on metabolic and lifestyle interventions. The study evaluates and compares single and combined control strategies to identify the most cost-effective approach for reducing the burden of TB–DM coinfection. Accordingly, this work develops a TB–DM coinfection model and assesses effective optimal control strategies through mathematical analysis and numerical simulations.

2. Methods

The research method began with a literature study related to mathematical models of tuberculosis-diabetes mellitus coinfection with optimal control. The research stages included: (1) constructing a compartmental TB–DM coinfection model based on epidemiologically justified assumptions; (2) determining the equilibrium points and deriving the basic reproduction number using the next-generation matrix method; (3) analyzing the dynamic behavior of the model through linearization and evaluation of the Jacobian matrix; (4) adding optimal control to the model; (5) formulating and solving the optimal control problem using Pontryagin's minimum principle; (6) performing numerical simulations using the fourth-order Runge-Kutta method and the Forward–Backward Sweep method; and (7) drawing conclusions based on the results of the analysis and simulations.

3. Results and Discussion

3.1. Tuberculosis-Diabetes Mellitus (TB-DM) Coinfection Model

This study modifies the TB model developed by [6] by adding treatment compartments for TB and TB–DM coinfection. Hence, this study proposes a TB-DM model comprising 10 compartments, namely the non-diabetic susceptible individual compartment $S_T(t)$, the non-diabetic latent individual compartment $L_T(t)$, the non-diabetic active TB individual compartment $I_T(t)$, the non-diabetic treated individual compartment $J_T(t)$, the compartment of recovered from TB (non-diabetic) $R_T(t)$, the compartment of susceptible diabetic individuals $S_{DT}(t)$, the compartment

of latent diabetic individuals $L_{DT}(t)$, the compartment of active diabetic TB individuals $I_{DT}(t)$, the compartment of treated diabetic individuals $J_{DT}(t)$, and the compartment of recovered from TB (but still diabetic) $R_{DT}(t)$.

The treatment compartments J_T and J_{DT} represent non-diabetic and diabetic individuals who are currently receiving anti-tuberculosis therapy. Incomplete and irregular TB treatment can lead to relapse, causing patients to return to the latent infection stage. In contrast, the recovered compartments R_T and R_{DT} represent individuals who have successfully completed the treatment and are considered non-infectious.

There are several assumptions for constructing the TB–DM model in this study, including:

1. Due to the extremely low incidence of neonatal diabetes (approximately 1 in 90,000 births [12]), the birth rate Λ is assumed to contribute only to S_T.
2. All individuals experience natural mortality at rate μ. Additionally, I_T face TB-induced mortality d_1, while I_{DT} face d_2, with $d_2 \geq d_1$ reflecting more severe outcomes in TB-DM patients [13]. Treated individuals also experience disease-related mortality: d_3 for J_T and d_4 for J_{DT}, with $d_4 \geq d_3$.
3. TB transmission occurs through effective contact with active cases. The force of infection is $\lambda_\beta = \frac{\beta(I_T+\varepsilon I_{DT})}{N}$, where $\varepsilon > 1$ denotes the increased infectiousness of diabetic TB cases. Susceptible individuals acquire infection at rates λ_β (non-diabetic) and $\theta\lambda_\beta$ (diabetic), with $\theta > 1$ capturing diabetes-related immune susceptibility [14].
4. Newly infected non-diabetic individuals enter L_T with probability q_1 and progress directly to I_T with probability $(1 - q_1)$. Similarly, newly infected diabetics enter L_{DT} with probability q_2 and progress to I_{DT} with probability $(1 - q_2)$.
5. Individuals in S_T, L_T, J_T, and R_T can develop diabetes and move to the corresponding diabetic classes at rate α. This transition represents the onset of diabetes driven by individual metabolic risk factors rather than infectious transmission. TB infection can induce stress-related hyperglycemia, and for people with underlying vulnerabilities, such as advanced age, obesity, family history of diabetes, high-sugar diet, or impaired glucose regulation, this condition may contribute to the development of diabetes [15]. Active TB individuals I_T can also develop diabetes at an elevated rate $\tau\alpha$ ($\tau > 1$), reflecting the additional metabolic burden associated with active TB.
6. Diabetes is a chronic condition with no cure. While glycemic control is achievable, individuals do not return to a non-diabetic state. Therefore, transitions from diabetic to non-diabetic compartments are excluded from the model. This biological irreversibility justifies the distinct clinical pathways for TB–DM patients.
7. Latent individuals in compartment L_T progress to I_T at rate δ_1 or are detected and start treatment (move to J_T) at rate η_1. Similarly, latent diabetic individuals in L_{DT} progress to I_{DT} at rate $\theta\delta_2$ or are detected and start treatment at rate η_2. Due to diabetes-related immune impairment and delayed case detection, we assume $\theta\delta_2 \geq \delta_1$ and $\eta_2 \leq \eta_1$.
8. Active TB individuals are detected and start treatment at rates γ_1 ($I_T \to J_T$) and γ_2 ($I_{DT} \to J_{DT}$). Although the standard treatment for drug-susceptible TB is identical for both groups, the TB–DM guidelines report slower response and higher risk of complications among diabetic patients [11]; thus the model assumes $\gamma_2 < \gamma_1$.
9. Treated individuals may recover or relapse. Those in J_T complete treatment and move to R_T at rate $p_1 r_1$, or experience treatment failure/relapse (returning to L_T) at rate $(1-p_1)r_1$. Similarly, J_{DT} individuals move to R_{DT} at rate $p_2 r_2$ or relapse to L_{DT} at rate $(1-p_2)r_2$. Clinical evidence suggests $p_2 \leq p_1$.

Eq. (1) shows a compartment diagram that illustrates the dynamics of TB-DM coinfection.

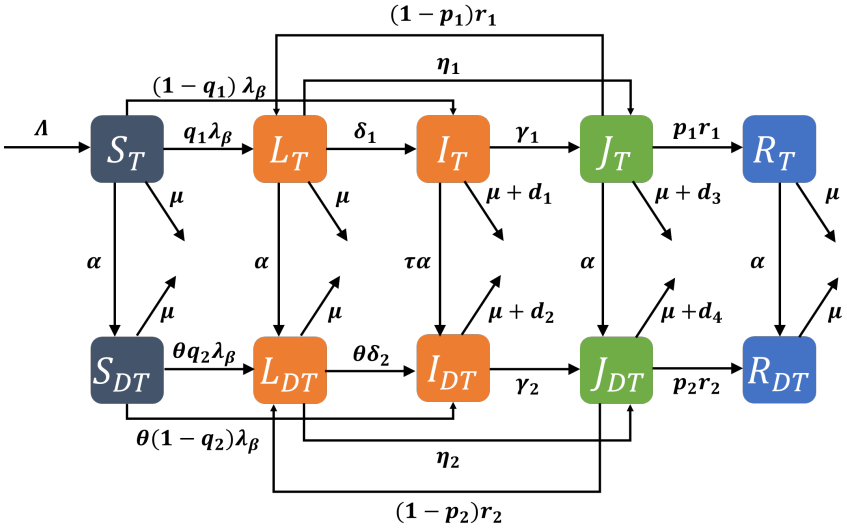

Figure 1: TB-DM Compartment Diagram

Based on the above assumptions, the transmission dynamics of TB–DM coinfection are described by the following system of differential equations:

$$\begin{aligned}
\frac{dS_T}{dt} &= \Lambda - \lambda_\beta S_T - (\alpha+\mu)S_T,\\
\frac{dL_T}{dt} &= q_1\lambda_\beta S_T - (\delta_1+\eta_1+\mu+\alpha)L_T + (1-p_1)r_1 J_T,\\
\frac{dI_T}{dt} &= (1-q_1)\lambda_\beta S_T + \delta_1 L_T - (\tau\alpha+\mu+d_1+\gamma_1)I_T,\\
\frac{dJ_T}{dt} &= \gamma_1 I_T + \eta_1 L_T - (r_1+\mu+d_3+\alpha)J_T,\\
\frac{dR_T}{dt} &= p_1 r_1 J_T - (\alpha+\mu)R_T,\\
\frac{dS_{DT}}{dt} &= \alpha S_T - \theta\lambda_\beta S_{DT} - \mu S_{DT},\\
\frac{dL_{DT}}{dt} &= \alpha L_T + \theta q_2\lambda_\beta S_{DT} - (\theta\delta_2+\eta_2+\mu)L_{DT} + (1-p_2)r_2 J_{DT},\\
\frac{dI_{DT}}{dt} &= \tau\alpha I_T + \theta(1-q_2)\lambda_\beta S_{DT} + \theta\delta_2 L_{DT} - (\gamma_2+\mu+d_2)I_{DT},\\
\frac{dJ_{DT}}{dt} &= \alpha J_T + \gamma_2 I_{DT} + \eta_2 L_{DT} - (r_2+\mu+d_4)J_{DT},\\
\frac{dR_{DT}}{dt} &= \alpha R_T + p_2 r_2 J_{DT} - \mu R_{DT},
\end{aligned} \tag{1}$$

with

$$\lambda_\beta = \frac{\beta(I_T+\varepsilon I_{DT})}{N} \quad \text{and} \quad N = S_T+L_T+I_T+J_T+R_T+S_{DT}+L_{DT}+I_{DT}+J_{DT}+R_{DT}.$$

The initial conditions are $S_T(0) \geq 0$, $L_T(0) \geq 0$, $I_T(0) \geq 0$, $J_T(0) \geq 0$, $R_T(0) \geq 0$, $S_{DT}(0) \geq 0$, $L_{DT}(0) \geq 0$, $I_{DT}(0) \geq 0$, $J_{DT}(0) \geq 0$, $R_{DT}(0) \geq 0$, and all parameters are assumed to be positive.

3.2. Dynamic Analysis

The equilibrium point of model Eq. (1) is a constant solution obtained when

$$\frac{dS_T}{dt} = \frac{dL_T}{dt} = \frac{dI_T}{dt} = \frac{dJ_T}{dt} = \frac{dR_T}{dt} = \frac{dS_{DT}}{dt} = \frac{dL_{DT}}{dt} = \frac{dI_{DT}}{dt} = \frac{dJ_{DT}}{dt} = \frac{dR_{DT}}{dt} = 0.$$

Table 1: Parameter Values

Parameter	Meaning	Value	Units
Λ	Natural birth rate	$\frac{1}{72.39}N$	individuals/year
β	Transmission rate	0.7	1/year
ε	Transmission adjustment factor or relative transmission effectiveness of infectious individuals with DM	1.1	-
α	Rate of transition of individuals from non-diabetic to diabetic status	0.009	1/year
τ	Risk factor for activation/transition of latent TB to infectious TB in individuals with DM	1.01	-
μ	Natural death rate	1/72.39	1/year
q_1, q_2	Proportion of individuals who enter the latent stage after exposure, with $0 \leq q_1, q_2 \leq 1$	0.9; 0.9	-
p_1, p_2	Proportion of individuals who recover after treatment, with $0 \leq p_1, p_2 \leq 1$	0.8; 0.7	-
δ_1, δ_2	Progression rate from latent TB to active TB	0.16; 0.1711	1/year
η_1, η_2	Treatment initiation rates for latent TB individuals (non-diabetic, diabetic)	0.01147; 0.00947	1/year
γ_1, γ_2	Treatment rate of non-diabetic and diabetic individuals, respectively	0.095; 0.075	1/year
$d_1, d_2,$ d_3, d_4	Disease-induced mortality rates	0.083; 1.25×0.083; 0.05; 1.25×0.05	1/year
θ	TB risk amplification factor	1.01	-
r_1, r_2	Recovery rate after treatment for non-diabetic and diabetic individuals, respectively	0.094; 0.08	1/year
N	Total Population	271686	individuals

so that it is obtained

$$\begin{aligned}
\Lambda - \lambda_\beta S_T - k_1 S_T &= 0 \\
q_1 \lambda_\beta S_T - k_2 L_T + k_3 J_T &= 0 \\
(1-q_1)\lambda_\beta S_T + \delta_1 L_T - k_4 I_T &= 0 \\
\gamma_1 I_T + \eta_1 L_T - k_5 J_T &= 0 \\
p_1 r_1 J_T - k_1 R_T &= 0 \\
\alpha S_T - \theta \lambda_\beta S_{DT} - \mu S_{DT} &= 0 \\
\alpha L_T + \theta q_2 \lambda_\beta S_{DT} - k_6 L_{DT} + k_7 J_{DT} &= 0 \\
\tau \alpha I_T + \theta(1-q_2)\lambda_\beta S_{DT} + \theta \delta_2 L_{DT} - k_8 I_{DT} &= 0 \\
\alpha J_T + \gamma_2 I_{DT} + \eta_2 L_{DT} - k_9 J_{DT} &= 0 \\
\alpha R_T + p_2 r_2 J_{DT} - \mu R_{DT} &= 0
\end{aligned} \tag{2}$$

with $k_1 = \alpha + \mu$, $k_2 = \delta_1 + \eta_1 + \mu + \alpha$, $k_3 = (1-p_1)r_1$, $k_4 = \tau\alpha + \mu + d_1 + \gamma_1$, $k_5 = r_1 + \mu + d_3 + \alpha$, $k_6 = \theta\delta_2 + \eta_2 + \mu$, $k_7 = (1-p_2)r_2$, $k_8 = \gamma_2 + \mu + d_2$, $k_9 = r_2 + \mu + d_4$.

3.2.1. Disease-Free Equilibrium Point and Basic Reproduction Number

If $\lambda_\beta = 0$ is substituted into system Eq. (2), then the disease-free equilibrium point is obtained as:

$$X^0 = (S_T^0, L_T^0, I_T^0, J_T^0, R_T^0, S_{DT}^0, L_{DT}^0, I_{DT}^0, J_{DT}^0, R_{DT}^0) = \left(\frac{\Lambda}{k_1}, 0, 0, 0, 0, \frac{\alpha\Lambda}{k_1\mu}, 0, 0, 0, 0\right).$$

Let $z \in \{L_T, I_T, J_T, L_{DT}, I_{DT}, J_{DT}\}$ denote the infected compartments of system Eq. (1).

Hence, for each infected state variable z, the dynamics can be written as $\dfrac{dz}{dt} = \mathcal{F} - \mathcal{V}$ with

$$\mathcal{F} = \frac{\beta(I_T + \varepsilon I_{DT})}{N} \begin{bmatrix} q_1 S_T \\ (1-q_1) S_T \\ 0 \\ \theta q_2 S_{DT} \\ \theta(1-q_2) S_{DT} \\ 0 \end{bmatrix} \quad \text{and} \quad \mathcal{V} = \begin{bmatrix} k_2 L_T - k_3 J_T \\ k_4 I_T - \delta_1 L_T \\ -\gamma_1 I_T + k_5 J_T - \eta_1 L_T \\ -\alpha L_T + k_6 L_{DT} - k_7 J_{DT} \\ -\tau\alpha I_T - \theta\delta_2 L_{DT} + k_8 I_{DT} \\ -\alpha J_T - \gamma_2 I_{DT} + k_9 J_{DT} - \eta_2 L_{DT} \end{bmatrix}.$$

The Jacobian matrices F and V are obtained by computing the partial derivatives of the entries of $\mathcal{F}$ and $\mathcal{V}$ with respect to $L_T,\ I_T,\ J_T,\ L_{DT},\ I_{DT},\ J_{DT}$ at X^0, namely:

$$F(X^0) = \frac{\Lambda\beta}{N k_1 \mu} \begin{bmatrix} 0 & q_1\mu & 0 & 0 & q_1\varepsilon\mu & 0 \\ 0 & (1-q_1)\mu & 0 & 0 & (1-q_1)\varepsilon\mu & 0 \\ 0 & 0 & 0 & 0 & 0 & 0 \\ 0 & \theta q_2 \alpha & 0 & 0 & \theta q_2 \varepsilon \alpha & 0 \\ 0 & \theta(1-q_2)\alpha & 0 & 0 & \theta(1-q_2)\varepsilon\alpha & 0 \\ 0 & 0 & 0 & 0 & 0 & 0 \end{bmatrix} \text{ and}$$

$$V(X^0) = \begin{bmatrix} k_2 & 0 & -k_3 & 0 & 0 & 0 \\ -\delta_1 & k_4 & 0 & 0 & 0 & 0 \\ -\eta_1 & -\gamma_1 & k_5 & 0 & 0 & 0 \\ -\alpha & 0 & 0 & k_6 & 0 & -k_7 \\ 0 & -\tau\alpha & 0 & -\theta\delta_2 & k_8 & 0 \\ 0 & 0 & -\alpha & -\eta_2 & -\gamma_2 & k_9 \end{bmatrix}.$$

The next generation matrix is defined as $G = F(X^0)\, V^{-1}(X^0)$. Thus, the basic reproduction number $\mathcal{R}_0$ is given by the spectral radius of the next generation matrix G.

$$\mathcal{R}_0 = \frac{\Lambda\beta}{\mu N k_1 m_1 m_4} \Big(\theta\alpha\varepsilon m_1 m_2 + \mu m_3 m_4 + \mu\alpha\varepsilon(\delta_2\theta m_5 + \tau m_3 m_6) \Big)$$

with

$$\begin{aligned}
m_1 &= \delta_1 k_5(\tau\alpha + \mu + d_1) + (\delta_1\gamma_1 + \eta_1 k_4)(p_1 r_1 + \alpha + \mu + d_3) + k_1 k_4 k_5 \\
m_2 &= (1-q_2)(p_2 r_2 + \mu + d_4)\eta_2 + ((1-q_2)\mu + \theta\delta_2) k_9 \\
m_3 &= \delta_1 q_1 k_5 + (1-q_1)(\delta_1 + \mu + \alpha) k_5 + (1-q_1)\eta_1(p_1 r_1 + \alpha + \mu + d_3) \\
m_4 &= p_2 r_2(\theta\delta_2\gamma_2 + \eta_2 k_8) + \theta\delta_2 r_2(\mu + d_2) + \mu k_8 r_2 + k_6 k_8(\mu + d_4) \\
m_5 &= q_1((\delta_1\gamma_1 + \eta_1 k_4) k_7 + k_4 k_5 k_9) + (1-q_1)\gamma_1(k_2 k_7 + k_3 k_9) \\
m_6 &= (\theta\delta_2 + \mu) k_9 + \eta_2(p_2 r_2 + \mu + d_4)
\end{aligned}$$

Hence, the basic reproduction number $\mathcal{R}_0$ represents the expected number of secondary active TB cases generated by a single infectious individual introduced into a fully susceptible population consisting of both diabetic and non-diabetic individuals. The value of $\mathcal{R}_0$ reflects the combined effects of TB transmission, increased infectiousness of TB–DM cases, heightened susceptibility among diabetic individuals, progression from latent to active TB, treatment initiation, recovery, relapse, and disease-induced mortality, which together determine the overall transmission potential of TB–DM coinfection.

3.2.2. Endemic Equilibrium Point

Based on equations Eq. (2), the following equilibrium point is obtained. The endemic equilibrium point is denoted by $X^* = (S_T^*, L_T^*, I_T^*, J_T^*, R_T^*, S_{DT}^*, L_{DT}^*, I_{DT}^*, J_{DT}^*, R_{DT}^*)$, with

$$S_T^* = \frac{\Lambda}{\lambda_\beta^* + k_1},$$

$$L_T^* = \frac{\Lambda q_1 k_5 \lambda_\beta^* + (1-p_1)\gamma_1 r_1 (\lambda_\beta^* + k_1) I_T^*}{(\lambda_\beta^* + k_1)(\eta_1(p_1 r_1 + d_3 + k_1) + (\delta_1 + k_1)k_5)},$$

$$I_T^* = \frac{\Lambda m_3 \lambda_\beta^*}{m_1(\lambda_\beta^* + k_1)},$$

$$J_T^* = \frac{L_T^* \eta_1 + I_T^* \gamma_1}{k_5},$$

$$R_T^* = \frac{p_1 r_1 J_T^*}{k_1},$$

$$S_{DT}^* = \frac{\alpha\Lambda}{(\lambda_\beta^* + k_1)(\theta\lambda_\beta^* + \mu)},$$

$$\begin{aligned} L_{DT}^* = \frac{\lambda_\beta^* \Lambda \alpha}{m_1 m_4 (\theta\lambda_\beta^* + \mu)(\lambda_\beta^* + k_1)} \Big(& (\lambda_\beta^*\theta + \mu)(q_1\tau\delta_1(d_3 + k_1)k_7\gamma_2 + \tau\delta_1 r_1 k_7 \gamma_2 + q_1\delta_1\gamma_1 k_7 k_8 \\ & + q_1\eta_1 k_4 k_7 k_8 + (1-q_1)\gamma_1 k_2 k_7 k_8 + (1-q_1)(1-p_1)\gamma_1 r_1 k_8 k_9 + q_1 k_4 k_5 k_8 k_9 \\ & + \tau(1-q_1)((d_3 + k_1)k_2 + (\eta_1 p_1 + k_1)r_1)k_7\gamma_2) + \theta m_1(q_2 k_8 k_9 + \gamma_2(1-q_2)k_7)\Big), \end{aligned}$$

$$I_{DT}^* = \frac{\alpha\Lambda\lambda_\beta^*((\theta\lambda_\beta^* + \mu)(\tau m_3 m_6 + \theta\delta_2 m_5) + \theta m_1(\theta\delta_2 k_9 + (1-q_2)(\mu k_9 + (p_2 r_2 + \mu + d_4)\eta_2)))}{m_1 m_4 (\theta\lambda_\beta^* + \mu)(\lambda_\beta^* + k_1)},$$

$$\begin{aligned} J_{DT}^* = & \frac{(q_1\eta_1\alpha\Lambda\lambda_\beta^* + ((\delta_1 + \mu + \alpha)k_5 + \eta_1(d_3 + \alpha + \mu) + p_1 r_1 \eta_1)((\lambda_\beta^* + k_1))(\gamma_2 I_{DT}^* + \eta_2 L_{DT}^*)}{(\lambda_\beta^* + k_1)(\eta_1(p_1 r_1 + \alpha + \mu + d_3) + (\delta_1 + \mu + \alpha)k_5)k_9} \\ & + \frac{(\lambda_\beta^* + k_1)\alpha\gamma_1 k_2 I_T^*)}{(\lambda_\beta^* + k_1)(\eta_1(p_1 r_1 + \alpha + \mu + d_3) + (\delta_1 + \mu + \alpha)k_5)k_9}, \end{aligned}$$

$$R_{DT}^* = \frac{\alpha R_T^* + p_2 r_2 J_{DT}^*}{\mu}.$$

Theorem 3.1 (Existence and Uniqueness of the Endemic Equilibrium)**.** *The system Eq. (1) has a unique endemic equilibrium point X^* if $\mathcal{R}_0 > 1$. Moreover, no endemic equilibrium exists when $\mathcal{R}_0 < 1$.*

Proof. The endemic equilibrium X^* exists if and only if $\lambda_\beta^* > 0$, where λ_β^* denotes the positive root of the following quadratic equation:

$$H(\lambda_\beta^*) = w_2(\lambda_\beta^*)^2 + w_1\lambda_\beta^* + w_0, \tag{3}$$

with

$$w_0 = Nk_1\mu m_1^2 m_4(1-\mathcal{R}_0),$$
$$w_1 = m_1^2\left(\frac{\Lambda\beta\theta^2\alpha\varepsilon m_2}{\mu} + m_4 N(\mu+\theta k_1(1-\mathcal{R}_0))\right),$$
$$w_2 = N\theta m_1^2 m_4.$$

Accordingly, w_2 is always positive, w_1 can be positive or negative, and w_0 is negative when $\mathcal{R}_0 > 1$. Based on Eq. (3), the condition for the existence of X^* is as follows:

i. There exists one endemic equilibrium when $\mathcal{R}_0 > 1$,
ii. There is no endemic equilibrium when $\mathcal{R}_0 < 1$ and $w_1 > 0$.

Therefore, system Eq. (1) has a unique endemic equilibrium point when $\mathcal{R}_0 > 1$. □

3.2.3. Local Stability of the Equilibrium Point

Since system Eq. (1) is autonomous and nonlinear, the local stability of its equilibrium points is investigated through linearization. The Jacobian matrix of system Eq. (1) evaluated at an arbitrary equilibrium point is given by

$$J = \begin{bmatrix}
-\lambda_\beta - k_1 & 0 & -\frac{\beta S_T}{N} & 0 & 0 & 0 & 0 & -\frac{\beta\varepsilon S_T}{N} & 0 & 0 \\
q_1\lambda_\beta & -k_2 & \frac{q_1\beta S_T}{N} & k_3 & 0 & 0 & 0 & \frac{q_1\beta\varepsilon S_T}{N} & 0 & 0 \\
(1-q_1)\lambda_\beta & \delta_1 & \frac{(1-q_1)\beta S_T}{N} - k_4 & 0 & 0 & 0 & 0 & \frac{(1-q_1)\beta\varepsilon S_T}{N} & 0 & 0 \\
0 & \eta_1 & \gamma_1 & -k_5 & 0 & 0 & 0 & 0 & 0 & 0 \\
0 & 0 & 0 & p_1 r_1 & -k_1 & 0 & 0 & 0 & 0 & 0 \\
\alpha & 0 & -\frac{\theta\beta S_{DT}}{N} & 0 & 0 & -\theta\lambda_\beta - \mu & 0 & -\frac{\theta\beta\varepsilon S_{DT}}{N} & 0 & 0 \\
0 & \alpha & \frac{\theta q_2\beta S_{DT}}{N} & 0 & 0 & \theta q_2\lambda_\beta & -k_6 & \frac{\theta q_2\beta\varepsilon S_{DT}}{N} & k_7 & 0 \\
0 & 0 & \tau\alpha + \frac{\theta(1-q_2)\beta S_{DT}}{N} & 0 & 0 & \theta(1-q_2)\lambda_\beta & \theta\delta_2 & \frac{\theta(1-q_2)\beta\varepsilon S_{DT}}{N} - k_8 & 0 & 0 \\
0 & 0 & 0 & \alpha & 0 & 0 & \eta_2 & \gamma_2 & -k_9 & 0 \\
0 & 0 & 0 & 0 & \alpha & 0 & 0 & 0 & p_2 r_2 & -\mu
\end{bmatrix}.$$

The eigenvalues of $J(X^0)$ and $J(X^*)$ are obtained by solving the corresponding characteristic equations, which are of high degree and difficult to solve analytically. Therefore, numerical analysis of eigenvalues is necessary to assess stability.

Theorem 3.2 (Local Stability of the Disease-Free Equilibrium). *The disease-free equilibrium X^0 of system Eq. (1) is locally asymptotically stable if $\mathcal{R}_0 < 1$ and unstable if $\mathcal{R}_0 > 1$. [16]*

The stability of the endemic equilibrium X^* when $\mathcal{R}_0 > 1$ is examined numerically in the following subsection using parameter values from Eq. (1).

3.2.4. Numerical Analysis of the Equilibrium Points

To complement the analytical results and examine the stability of the endemic equilibrium, numerical computations are performed using the parameter values listed in Eq. (1). Two cases are considered: $\mathcal{R}_0 < 1$ to verify Eq. (3.2), and $\mathcal{R}_0 > 1$ to investigate the existence and stability of the endemic equilibrium.

Case 1: Numerical verification for $\mathcal{R}_0 < 1$. To verify Theorem 1 (stability of the DFE when $\mathcal{R}_0 < 1$), we set $\beta = 0.1$, which gives $\mathcal{R}_0 = 0.513$. The corresponding disease-free equilibrium is

$$X^0 = (164507.63, 0, 0, 0, 0, 107178.37, 0, 0, 0, 0).$$

The eigenvalues of the Jacobian matrix evaluated at X^0 are:

$$\lambda_1 = -0.023 + 8.88 \times 10^{-8} i, \quad \lambda_2 = -0.226 + 0.056i, \quad \lambda_3 = -0.014, \quad \lambda_4 = -0.014, \quad \lambda_5 = -0.049,$$
$$\lambda_6 = -0.023 - 8.88 \times 10^{-8} i, \quad \lambda_7 = -0.226 - 0.056i \quad \lambda_8 = -0.120, \quad \lambda_9 = -0.174, \quad \lambda_{10} = -0.302.$$

All eigenvalues have negative real parts, confirming numerically that the disease-free equilibrium is locally asymptotically stable when $\mathcal{R}_0 < 1$.

Case 2: For $\mathcal{R}_0 > 1$. Using the full set of baseline parameters from Table 1 (with $\beta = 0.7$), we obtain $\mathcal{R}_0 = 3.592 > 1$. The endemic equilibrium is computed as

$$X^* = (65558.4,\ 11079.2,\ 9947.1,\ 6426.6,\ 21183.6,\ 12142.3,\ 2694.4,\ 3106.8,\ 2023.9,\ 22005.9).$$

The eigenvalues of the Jacobian matrix evaluated at X^* are:

$$\lambda_1 = -0.022 + 0.053i,, \quad \lambda_2 = -0.229 + 0.056i, \quad \lambda_3 = -0.143 + 0.02i, \quad \lambda_4 = -0.014, \quad \lambda_5 = -0.023,$$
$$\lambda_6 = -0.022 - 0.053i, \quad \lambda_7 = -0.229 - 0.056i \quad \lambda_8 = -0.143 - 0.02i, \quad \lambda_9 = -0.049, \quad \lambda_{10} = -0.356.$$

All eigenvalues again have negative real parts. Hence, for this representative parameter set yielding $\mathcal{R}_0 > 1$, the numerical computation indicates that the endemic equilibrium is locally asymptotically stable.

The numerical results corroborate the theoretical threshold behavior: when $\mathcal{R}_0 < 1$ the disease-free equilibrium is stable and the disease dies out, while for $\mathcal{R}_0 > 1$ a unique endemic equilibrium exists and is numerically stable for the considered parameter values. This persistent endemic state under baseline parameters motivates the design of control strategies analyzed in the subsequent section.

3.3. Optimal Control Characterization

The optimal control strategy aims to reduce the number of individuals infected with tuberculosis and TB–DM coinfection while minimizing the associated implementation costs. The objective functional is defined as

$$J(u_1, u_2) = \int_0^{t_f} \left(A_1 I_T + A_2 I_{DT} + A_3 J_T + A_4 J_{DT} + \frac{B_1}{2} u_1^2 + \frac{B_2}{2} u_2^2 \right) dt \tag{4}$$

with nonnegative initial conditions. A_1, A_2, A_3, and A_4 are positive weight constants associated with the infected compartments I_T, I_{DT}, J_T, and J_{DT}, respectively. B_1 and B_2 are positive weight constants associated with the control measures u_1 (TB transmission reduction) and u_2 (diabetes prevention), respectively. The optimal control problem is to find admissible control functions (u_1^*, u_2^*) that minimize

$$J(u_1^*, u_2^*) = \min_U \{J(u_1, u_2)\},$$

with $U = \{(u_1, u_2) \mid 0 \le u_i \le 1,\ t \in [0, t_f],\ i = 1, 2\}$.

To characterize an optimal solution, we begin by defining the Hamilton function as follows:

$$\begin{aligned}
H = {} & A_1 I_T + A_2 I_{DT} + A_3 J_T + A_4 J_{DT} + \frac{B_1}{2} u_1^2 + \frac{B_2}{2} u_2^2 \\
& + \lambda_1 \left(\Lambda - (1-u_1)\lambda_\beta S_T - ((1-u_2)\alpha + \mu) S_T \right), \\
& + \lambda_2 \left(q_1 (1-u_1)\lambda_\beta S_T - (\delta_1 + \eta_1 + \mu + (1-u_2)\alpha) L_T + (1-p_1) r_1 J_T \right), \\
& + \lambda_3 \left((1-q_1)(1-u_1)\lambda_\beta S_T + \delta_1 L_T - (\tau(1-u_2)\alpha + \mu + d_1 + \gamma_1) I_T \right), \\
& + \lambda_4 \left(\gamma_1 I_T + \eta_1 L_T - (r_1 + \mu + d_3 + (1-u_2)\alpha) J_T \right), \\
& + \lambda_5 \left(p_1 r_1 J_T - ((1-u_2)\alpha + \mu) R_T \right), \\
& + \lambda_6 \left((1-u_2)\alpha S_T - \theta(1-u_1)\lambda_\beta S_{DT} - \mu S_{DT} \right), \\
& + \lambda_7 \left((1-u_2)\alpha L_T + \theta q_2 (1-u_1)\lambda_\beta S_{DT} - (\theta\delta_2 + \eta_2 + \mu) L_{DT} + (1-p_2) r_2 J_{DT} \right), \\
& + \lambda_8 \left(\tau(1-u_2)\alpha I_T + \theta(1-q_2)(1-u_1)\lambda_\beta S_{DT} + \theta\delta_2 L_{DT} - (\gamma_2 + \mu + d_2) I_{DT} \right),
\end{aligned}$$

$$+\lambda_9\left((1-u_2)\alpha J_T+\gamma_2 I_{DT}+\eta_2 L_{DT}-(r_2+\mu+d_4)J_{DT}\right),$$
$$+\lambda_{10}\left((1-u_2)\alpha R_T+p_2 r_2 J_{DT}-\mu R_{DT}\right).$$

where $\lambda_i(t)$, $i=1,\ldots,10$ are the costate variables associated with the state variables S_T, L_T, I_T, J_T, R_T, S_{DT}, L_{DT}, I_{DT}, J_{DT}, R_{DT}, respectively.

Using the conditions from Pontryagin's minimum principle [9], we obtain the state system, the costate system, and optimal control solution. The state system is derived by taking the partial derivatives of the Hamiltonian H with respect to each costate variable, as follows

$$\begin{aligned}
\frac{dS_T}{dt} &= \Lambda-(1-u_1)\lambda_\beta S_T-((1-u_2)\alpha+\mu)S_T,\\
\frac{dL_T}{dt} &= q_1(1-u_1)\lambda_\beta S_T-(\delta_1+\eta_1+\mu+(1-u_2)\alpha)L_T+(1-p_1)r_1J_T,\\
\frac{dI_T}{dt} &= (1-q_1)(1-u_1)\lambda_\beta S_T+\delta_1 L_T-(\tau(1-u_2)\alpha+\mu+d_1+\gamma_1)I_T,\\
\frac{dJ_T}{dt} &= \gamma_1 I_T+\eta_1 L_T-(r_1+\mu+d_3+(1-u_2)\alpha)J_T,\\
\frac{dR_T}{dt} &= p_1r_1J_T-((1-u_2)\alpha+\mu)R_T,\\
\frac{dS_{DT}}{dt} &= (1-u_2)\alpha S_T-\theta(1-u_1)\lambda_\beta S_{DT}-\mu S_{DT},\\
\frac{dL_{DT}}{dt} &= (1-u_2)\alpha L_T+\theta q_2(1-u_1)\lambda_\beta S_{DT}-(\theta\delta_2+\eta_2+\mu)L_{DT}+(1-p_2)r_2J_{DT},\\
\frac{dI_{DT}}{dt} &= \tau(1-u_2)\alpha I_T+\theta(1-q_2)(1-u_1)\lambda_\beta S_{DT}+\theta\delta_2 L_{DT}-(\gamma_2+\mu+d_2)I_{DT},\\
\frac{dJ_{DT}}{dt} &= (1-u_2)\alpha J_T+\gamma_2 I_{DT}+\eta_2 L_{DT}-(r_2+\mu+d_4)J_{DT},\\
\frac{dR_{DT}}{dt} &= (1-u_2)\alpha R_T+p_2r_2J_{DT}-\mu R_{DT},
\end{aligned}\tag{5}$$

The costate system is derived by taking the partial derivatives of the Hamiltonian H with respect to each state variable, yielding the following expressions:

$$\begin{aligned}
\frac{d\lambda_1}{dt} &= -\frac{\partial H}{\partial S_T} = \lambda_1\left((1-u_1)\lambda_\beta+(1-u_2)\alpha+\mu\right)-\lambda_2 q_1(1-u_1)\lambda_\beta\\
&\quad-\lambda_3(1-q_1)(1-u_1)\lambda_\beta-\lambda_6(1-u_2)\alpha
\end{aligned}$$

$$\frac{d\lambda_2}{dt} = -\frac{\partial H}{\partial L_T} = \lambda_2(\delta_1+\eta_1+\mu+(1-u_2)\alpha)-\lambda_3\delta_1-\lambda_4\eta_1-\lambda_7(1-u_2)\alpha$$

$$\begin{aligned}
\frac{d\lambda_3}{dt} &= -\frac{\partial H}{\partial I_T} = -A_1+\frac{\lambda_1\beta(1-u_1)S_T}{N}-\frac{\lambda_2 q_1\beta(1-u_1)S_T}{N}-\frac{\lambda_3(1-q_1)\beta(1-u_1)S_T}{N}\\
&\quad+\lambda_3((1-u_2)\tau\alpha+\mu+d_1+\gamma_1)-\lambda_4\gamma_1+\frac{\lambda_6\theta\beta(1-u_1)S_{DT}}{N}\\
&\quad-\frac{\lambda_7\theta q_2\beta(1-u_1)S_{DT}}{N}-\lambda_8\left(\frac{\theta(1-q_2)\beta(1-u_1)S_{DT}}{N}+(1-u_2)\tau\alpha\right)
\end{aligned}$$

$$\frac{d\lambda_4}{dt} = -\frac{\partial H}{\partial J_T} = -A_3-\lambda_2(1-p_1)r_1+\lambda_4(r_1+\mu+d_3+(1-u_2)\alpha)-\lambda_5 p_1 r_1-\lambda_9(1-u_2)\alpha$$

$$\frac{d\lambda_5}{dt} = -\frac{\partial H}{\partial R_T} = \lambda_5((1-u_2)\alpha+\mu)-\lambda_{10}(1-u_2)\alpha$$

$$\frac{d\lambda_6}{dt} = -\frac{\partial H}{\partial S_{DT}} = \lambda_6\left(\theta(1-u_1)\lambda_\beta+\mu\right)-\lambda_7\theta q_2(1-u_1)\lambda_\beta-\lambda_8\theta(1-q_2)(1-u_1)\lambda_\beta$$

$$\frac{d\lambda_7}{dt} = -\frac{\partial H}{\partial L_{DT}} = \lambda_7(\theta\delta_2 + \mu + \eta_2) - \lambda_8\theta\delta_2 - \lambda_9\eta_2$$

$$\begin{aligned}\frac{d\lambda_8}{dt} = -\frac{\partial H}{\partial I_{DT}} = -A_2 &+ \frac{\lambda_1\beta\varepsilon(1-u_1)S_T}{N} - \frac{\lambda_2 q_1\beta\varepsilon(1-u_1)S_T}{N} - \frac{\lambda_3(1-q_1)\beta\varepsilon(1-u_1)S_T}{N} \\ &+ \frac{\lambda_6\theta\beta\varepsilon(1-u_1)S_{DT}}{N} + \frac{\lambda_7\theta q_2\beta\varepsilon(1-u_1)S_{DT}}{N} - \frac{\lambda_8\theta(1-q_2)\beta\varepsilon(1-u_1)S_{DT}}{N} \\ &+ \lambda_8(\gamma_2 + \mu + d_2) - \lambda_9\gamma_2\end{aligned}$$

$$\frac{d\lambda_9}{dt} = -\frac{\partial H}{\partial J_{DT}} = -A_4 - \lambda_7(1-p_2)r_2 + \lambda_9(r_2 + \mu + d_4) - \lambda_{10}p_2 r_2$$

$$\frac{d\lambda_{10}}{dt} = -\frac{\partial H}{\partial R_{DT}} = \lambda_{10}\mu$$

with transversality condition $\lambda_i(t_f) = 0, \quad i = 1, 2, 3 \ldots 10.$

The optimal controls u_1 and u_2 are characterized by the stationary conditions $\dfrac{\partial H}{\partial u_1} = 0$ and $\dfrac{\partial H}{\partial u_2} = 0$, yielding

$$u_1^\dagger = \frac{\lambda_\beta(q_2\theta S_{DT}(\lambda_7 - \lambda_8) + \theta S_{DT}(\lambda_8 - \lambda_6) + q_1 S_T(\lambda_2 - \lambda_3) + S_T(\lambda_3 - \lambda_1))}{B_1}$$

$$u_2^\dagger = \frac{\alpha(\tau I_T(\lambda_8 - \lambda_3) + J_T(\lambda_9 - \lambda_4) + L_T(\lambda_7 - \lambda_2) + R_T(\lambda_{10} - \lambda_5) + S_T(\lambda_6 - \lambda_1))}{B_2}$$

Hence, the optimal controls u_i^*, $i = 1, 2$, subject to the bounds $0 \le u_i \le 1$, are characterized by

$$u_1^* = \min\left\{\max\left\{0, u_1^\dagger\right\}, 1\right\}$$

$$u_2^* = \min\left\{\max\left\{0, u_2^\dagger\right\}, 1\right\}$$

3.4. Numerical Simulation of the Optimal Control Strategies

To evaluate the effectiveness of the proposed optimal control strategies, system Eq. (5) was numerically solved using a combination of the fourth-order Runge–Kutta method and the Forward–Backward Sweep algorithm. The time variable is measured in years because tuberculosis and TB–DM coinfection are chronic diseases with slow progression and long treatment durations. Additionally, all model parameters are defined on an annual basis, ensuring dimensional consistency and alignment with epidemiological data.

The simulations were carried out using the initial conditions $S_T(0) = 190250$, $L_T(0) = 16500$, $I_T(0) = 10576$, $J_T(0) = 3500$, $R_T(0) = 810$, $S_{DT}(0) = 44870$, $L_{DT}(0) = 4000$, $I_{DT}(0) = 1000$, $J_{DT}(0) = 100$, $R_{DT}(0) = 80$, together with the parameter values listed in Eq. (1). The weight constants in the objective functional were chosen as $A_1 = 10$, $A_2 = 20$, $A_3 = 1$, $A_4 = 1$, $B_1 = 40000$, $B_2 = 200$. Simulation results of system Eq. (5) under different control strategies, namely no control, u_1 only, u_2 only, and combined controls (u_1, u_2), are presented in Eq. (2) and Eq. (3).

Under the u_1**-only strategy**, which reduces the effective contact rate β, a substantial reduction is observed in TB-only compartments. Eq. (2)(b)–(e) show that L_T, I_T, J_T, and R_T decrease significantly compared to the no-control scenario. A reduction is also observed in the TB–DM compartments (Eq. (2)(g)–(j)); however, the magnitude of reduction is smaller than that achieved under the combined control strategy. Meanwhile, Eq. (2)(a) and Eq. (2)(f) show a marked increase in the susceptible compartments S_T and S_{DT}, reflecting reduced new TB infections due to transmission control.

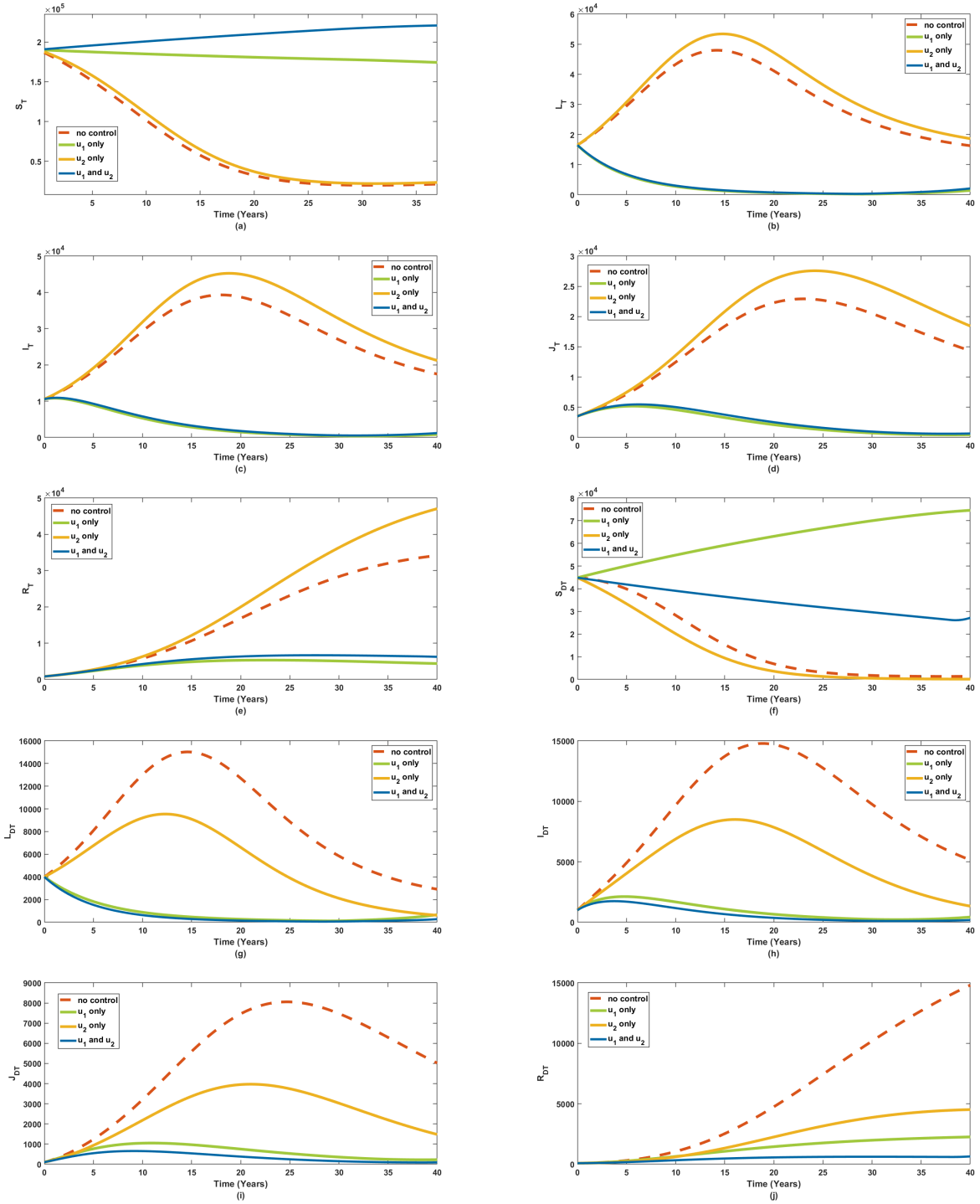

Figure 2: Simulation result of the model Eq. (5) under different strategies: no control, u_1 control only, u_2 control only, and combined controls (u_1, u_2)

In contrast, the u_2-only strategy targets the reduction of the diabetes onset rate α among TB-infected individuals. Eq. (2)(a)–(e) indicate only minor changes in S_T, L_T, I_T, J_T, R_T compartments, suggesting that u_2 alone is not effective in suppressing TB transmission. However, Eq. (2)(f)–(j) show a marked reduction in S_{DT}, L_{DT}, I_{DT}, J_{DT}, R_{DT} compartments, confirming that the u_2-only strategy primarily mitigates TB–DM progression rather than TB itself.

Under the combined control strategy (u_1, u_2), the largest reduction is observed in all infection-related compartments. As shown in Eq. (2)(b)–(e) and Eq. (2)(g)–(j), the compartments of L_T, I_T, J_T, R_T and their TB–DM counterparts $L_{DT}, I_{DT}, J_{DT}, R_{DT}$ decrease significantly.

Conversely, Eq. (2)(a) and Eq. (2)(f) show increased levels of S_T and S_{DT}, indicating effective suppression of new infections and disease progression.

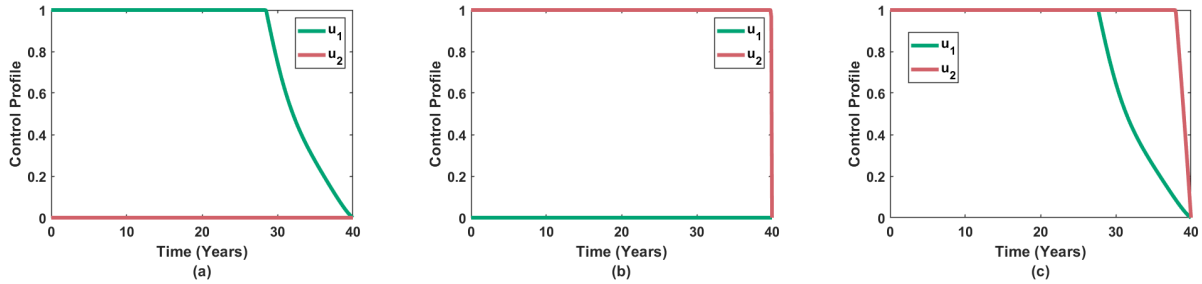

Figure 3: Simulation result of the corresponding optimal control profiles

The corresponding optimal control profiles are illustrated in Eq. (3). Eq. (3)(a) represents the u_1-only strategy, where $u_2(t) = 0$ for all t. The control $u_1(t)$ is applied at its maximum level during the early intervention period and gradually decreases as time approaches $t = 28.4$ years. In Eq. (3)(b), the control $u_1(t)$ does not appear because it is identically zero over the entire time interval, corresponding to the u_2-only strategy. The profile $u_2(t) = 1$ for $t \in [0, 39.7]$ indicates that maintaining the maximum level of diabetes prevention is optimal throughout most of the intervention period, reflecting the high susceptibility of TB-infected individuals to diabetes and the relatively lower cost associated with u_2. Eq. (3)(c) depicts the combined control strategy, in which both $u_1(t)$ and $u_2(t)$ are applied simultaneously at their maximum levels during the early phase. The control $u_1(t)$ begins to decline at approximately $t = 27.6$ years, while $u_2(t)$ remains maximal for a longer duration and starts to decrease at approximately $t = 37.9$ years. This behavior indicates that TB transmission control can be gradually relaxed once the infection burden is reduced, whereas diabetes prevention among TB-infected individuals requires sustained intervention.

Table 2: Objective function values under different control strategies

u_1 only	u_2 only	combined controls (u_1, u_2)
2.771×10^6	1.766×10^7	2.656×10^6

Furthermore, Eq. (2) presents the objective function values obtained under different control strategies. Since the aim of this study is to minimize the objective function given in Eq. (4), the combined control strategy (u_1, u_2) yields the smallest objective function value among all considered strategies.

Overall, the combined control strategy (u_1, u_2) is the most effective among all considered scenarios, as it simultaneously minimizes TB and TB–DM infections while optimizing the total intervention cost. These results are in concordance with established public health evidence, which underscores that case detection, isolation, contact tracing, behavioral education, and environmental protective interventions constitute core components of effective TB prevention [17]. Moreover, the findings are supported by [18] who demonstrated that lifestyle modifications among individuals with DM, such as increased physical activity, smoking cessation, and reduced alcohol consumption, can lower the risk of TB among individuals with diabetes mellitus. Consequently, the integration of these control measures can be regarded as a highly effective and evidence, based approach for mitigating TB–DM transmission and enhancing the efficiency of disease control programs.

4. Conclusion

This study developed a ten-compartment mathematical model to analyze the transmission dynamics of TB–DM coinfection. The analytical results show that the disease persists when

$\mathcal{R}_0 > 1$, which is consistent with the numerical estimate $\mathcal{R}_0 = 3.592$, confirming the potential for endemic persistence. Optimal control analysis incorporating two interventions, TB transmission reduction (u_1) and diabetes prevention among non-diabetic individuals (u_2), demonstrated that the combined strategy yields the most effective outcome. Numerical simulations showed that simultaneous implementation of both controls achieves the lowest objective function value (2.656×10^6), significantly reduces infected populations, and maintains higher susceptible levels compared to single-control approaches. These findings highlight the importance of integrated TB and DM prevention strategies to support more effective public health policies.

CRediT Authorship Contribution Statement

Muna Afdi Muniroh: Conceptualization, Methodology, Formal Analysis, Writing–Original Draft, **Kresna Oktafianto:** Writing–Review and Editing. **Eriska Fitri Kurniawati:** Project Administration and writing

Declaration of Generative AI and AI-assisted technologies

In preparing this manuscript, assistance from language-editing tools (ChatGPT and QuillBot) was used to improve clarity and grammar.

Declaration of Competing Interest

The authors declare no competing interest.

Funding and Acknowledgments

This research was funded by the Research Institute (LEMLIT) DIPA of the University of PGRI Ronggolawe in 2025 under the PPP scheme, with contract number 45/SP2H/PPP/Lemlit-Unirow/IV/2025.

Data and Code Availability

Not applicable.

References

[1] World Health Organization, *Global tuberculosis report 2024*, https://www.who.int/publications/i/item/9789240101531, 2024.

[2] C. for Disease Control and Prevention, *Preventing tuberculosis*, https://www.cdc.gov/tb/prevention/index.html, 2024.

[3] R. Amelia, I. I. Fujiati, D. Lindarto, E. Yunir, and H. Kusnanto, "Profile of tuberculosis patients with comorbid diabetes mellitus in medan, indonesia: A cross-sectional study," *PanAfrican Medical Journal*, vol. 24, pp. 49–54, 2023. DOI: 10.11604/pamj.2024.49.54.36492.

[4] Nursamsi, S. Toaha, and Kasbawati, "Stability analysis of tuberculosis spread model in diabetes mellitus patients with treatment factor," *Jurnal Matematika, Statistika, dan Komputasi*, vol. 17, no. 1, pp. 50–60, 2020. DOI: 10.20956/jmsk.v17i1.10245.

[5] S. F. Awad, J. A. Critchley, and L. J. Abu-Raddad, "Impact of diabetes mellitus on tuberculosis epidemiology in indonesia: A mathematical modeling analysis," *Tuberculosis*, vol. 134, p. 102 164, 2022. DOI: 10.1016/j.tube.2022.102164.

[6] J. D. Pratama and A. H. Permatasari, "Dynamic model of tuberculosis with diabetes mellitus," *Advances in Dynamical Systems and Applications*, vol. 18, no. 2, pp. 137–154, 2023.

[7] M. Dhara, V. Baths, and P. Danumjaya, "Mathematical modeling and dynamics of tuberculosis infection among diabetic patients in india," *The Journal of Analysis*, vol. 27, no. 2, pp. 451–463, 2018. DOI: 10.1007/s41478-018-0086-5.

[8] D. A. Maulina and C. Imron, "Analysis and optimal control of tuberculosis disease spread model with vaccination and case finding control (case study: Surabaya city)," *Barekeng: Jurnal Ilmu Matematika dan Terapan*, vol. 18, no. 2, pp. 1189–1200, 2024.

[9] M. A. Muniroh, Trisilowati, and W. M. Kusumawinahyu, "Optimal control of hepatitis b virus-induced liver cirrhosis model," *AIP Conference Proceedings*, vol. 2733, no. 1, p. 030 005, Jun. 2023. DOI: 10.1063/5.0140637. eprint: https://pubs.aip.org/aip/acp/article-pdf/doi/10.1063/5.0140637/18020697/030005_1_5.0140637.pdf. https://doi.org/10.1063/5.0140637.

[10] C. O. Agwu, "Mathematical model of the co-dynamics of diabetes and tuberculosis," Unpublished Doctoral Thesis, Ph.D. dissertation, Federal University of Technology, Owerri, Nigeria, 2023.

[11] Y. Lin et al., *Management of Diabetes Mellitus–Tuberculosis: A Guide to the Essential Practice*. Paris, France / Bagsværd, Denmark: The Union & World Diabetes Foundation, 2019. https://theunion.org/sites/default/files/2020-11/TheUnion_DMTB_Guide.pdf.

[12] J. Beltrand et al., "Neonatal diabetes mellitus," *Frontiers in Pediatrics*, vol. 8, p. 540 718, 2020. DOI: 10.3389/fped.2020.540718.

[13] V. Mave et al., "Diabetes mellitus and tuberculosis treatment outcomes in pune, india," *Open Forum Infectious Diseases*, vol. 8, 2021. DOI: 10.1093/ofid/ofab097.

[14] P. M. Thong, Y. H. Wong, H. Kornfeld, D. Goletti, and C. W. M. Ong, "Immune dysregulation of diabetes in tuberculosis.," *Seminars in immunology*, vol. 78, p. 101 959, 2025. DOI: 10.1016/j.smim.2025.101959.

[15] M. Bisht, P. Dahiya, S. Ghosh, and S. Mukhopadhyay, "The cause–effect relation of tuberculosis on incidence of diabetes mellitus," *Frontiers in Cellular and Infection Microbiology*, vol. 13, 2023. DOI: 10.3389/fcimb.2023.1134036.

[16] P. van den Driessche and J. Watmough, "Reproduction numbers and sub-threshold endemic equilibria for compartmental models of disease transmission," *Mathematical Biosciences*, vol. 180, no. 1–2, pp. 29–48, 2002. DOI: 10.1016/S0025-5564(02)00108-6.

[17] World Health Organization, *Preventing tuberculosis*, www.who.int/activities/preventing-tb, 2025.

[18] J. Park, J. H. Yoon, H. K. Ki, K. Han, and H. Kim, "Lifestyle changes and risk of tuberculosis in patients with type 2 diabetes mellitus: A nationwide cohort study," *Frontiers in Endocrinology*, vol. 13, p. 1 009 493, 2022. DOI: 10.3389/fendo.2022.1009493.